Continuum-model acoustic and electronic properties for a Fibonacci superlattice

A. H. MacDonald* and G. C. Aers
Division of Physics, National Research Council, Ottawa, Canada K1A 0R6
(Received 18 May 1987)

A continuum model is used to study the properties of acoustic phonons and of electrons in a semiconductor Fibonacci superlattice. Close contact is made with previous work based on discrete models by using a transfer-matrix approach. The mapping of transfer-matrix traces under the inflation transformation which defines the Fibonacci sequence has an invariant I, which has been identified as a key parameter in characterizing the Cantor-set spectra. We derive analytic expressions for the dependence of I on phonon frequency or electron energy and comment on the qualitative differences between discrete and continuum models. Transport properties are also discussed.

Interest in the spectral properties of one-dimensional (1D) quasiperiodic Schrödinger operators[1] has recently been reinvigorated by the discovery of quasicrystals.[2] In particular, Merlin *et al.*[3] realized that semiconductor quasiperiodic Fibonacci superlattices, which are related to the model for quasicrystals proposed by Levine and Steinhardt,[4] could be fabricated using molecular-beam-epitaxy (MBE) techniques. These developments led many workers[5–13] to reexamine the discrete Fibonacci chains which had been studied earlier by Kohmoto *et al.*[14] and independently by Ostlund *et al.*[15] In this paper we report on a study of Fibonacci superlattices using a continuum model which is known to provide an accurate description of either acoustic phonons or conduction electrons in a semiconductor superlattice. Unlike earlier studies, our work is directly relevant to MBE-fabricated Fibonacci superlattices.

We consider a set of points, $\{x_n\}$, along the MBE growth axis of a semiconducting film and separated by intervals of width d_A and d_B. All A intervals are filled with identical thin films, and all B intervals with a different set of identical films. The A intervals and B intervals occur in a Fibonacci sequence, which is defined by the following recursion relation: $S_1=B$, $S_2=A$; $S_j=S_{j-1}S_{j-2}$ for $j\geq 3$. For conduction electrons, the effective-mass approximation[16] leads to the Schrödinger equation

$$\frac{-\hbar^2}{2m^*}\frac{d^2\Psi}{dx^2}+V(x)\Psi(x)=E\Psi(x)\ , \tag{1}$$

where x is the coordinate along the growth direction and $V(x)$ is the conduction-band minimum. $V(x)$ is defined by the MBE growth prescription and may be taken, for the moment, to be some arbitrary function in the A and B intervals. Following Kohmoto[17] we introduce a transfer matrix by defining an interval of width 2ε, which we can subsequently set to zero, centered on each x_n where $V(x)=E_0$. then

$$\Psi(x)=\hat{\psi}_n e^{ik(x-x_n)}+\hat{\phi}_n e^{-ik(x-x_n)},\quad |x-x_n|\leq\epsilon \tag{2}$$

$E-E_0=\hbar^2k^2/2m^*$, and[18]

$$\begin{bmatrix}\hat{\phi}_{n+1}\\ \hat{\phi}_{n+1}\end{bmatrix}=\begin{bmatrix}u_n^* & -v_n^*\\ -v_n & u_n\end{bmatrix}\begin{bmatrix}\hat{\phi}_n\\ \hat{\phi}_n\end{bmatrix}\equiv\hat{M}_n\begin{bmatrix}\hat{\phi}_n\\ \hat{\phi}_n\end{bmatrix}\ . \tag{3}$$

In Eq. (3) $u_n=1/t_n$, $v_n=r_n/t_n$, and r_n and t_n are the reflection and transmission amplitudes through the barrier between x_n and x_{n+1} for a wave incident from the left. The form for Eq. (3) follows from time-reversal invariance and the conservation of probability [$|r_n|^2+|t_n|^2=1$ which implies that $\det(\hat{M}_n)=|u_n|^2-|v_n|^2=1$. We have assumed that E_0 is chosen so that k is real].

There is obviously a great deal of freedom in how the transfer matrix is defined and we take advantage of this to simplify some of the subsequent calculations. For example, changing E_0 to E_0' changes k to k' ($E-E_0'=\hbar^2k'^2/2m^*$), and u_n and v_n to u_n' and v_n'.

$$u_n'=(\alpha^2-\beta^2)^{-1}[\alpha^2u_n-\beta^2u_n^*+\alpha\beta(v_n-v_n^*)] \tag{4a}$$

and

$$v_n'=(\alpha^2-\beta^2)^{-1}[\alpha^2v_n-\beta^2v_n^*+\alpha\beta(u_n-u_n^*)]\ , \tag{4b}$$

where $\alpha=\frac{1}{2}+k/2k'$ and $\beta=\frac{1}{2}-k/2k'$. Similarly, we can write

$$\Psi(x)=\psi_n\cos[k(x-x_n)]+\phi_n\sin[k(x-x_n)] \tag{5a}$$

and define a transfer matrix so that

$$\begin{bmatrix}\phi_{n+1}\\ \phi_{n+1}\end{bmatrix}\equiv M_n\begin{bmatrix}\phi_n\\ \phi_n\end{bmatrix}\ . \tag{5b}$$

In this case Eq. (3) can be used to show that[19]

$$M_n=\begin{bmatrix}\mathrm{Re}(u_n-v_n) & -\mathrm{Im}(u_n+v_n)\\ \mathrm{Im}(u_n-v_n) & \mathrm{Re}(u_n+v_n)\end{bmatrix}\ . \tag{6}$$

As we see below, however, the spectral properties depend only on transfer-matrix traces and these must be independent of the specific definition used.

The Fibonacci superlattice is completely characterized by the transmission and reflection coefficients for A and

B intervals and we define $u_X \equiv 1/t_X$ and $v_X \equiv r_X/t_X$ where X is A or B. From the definition of the Fibonacci sequences it follows that the transfer matrices obey the recursion relation

$$\hat{T}_j = \hat{T}_{j-2}\hat{T}_{j-1}, \quad j \geq 3 \tag{7}$$

where $\hat{T}_1 = \hat{M}_B$, $\hat{T}_2 = \hat{M}_A$ and

$$\hat{T}_j = \hat{M}_{F_j}\hat{M}_{F_j-1} \cdots \hat{M}_1 \equiv \begin{bmatrix} w_j^* & -y_j^* \\ -y_j & w_j \end{bmatrix} \tag{8}$$

is the transfer matrix between from the beginning to the end of the jth generation of the Fibonacci sequence.[20] Writing $\hat{T}_{j-2} = \hat{T}_j \hat{T}_{j-1}^{-1}$ and noting that

$$\hat{T}_j^{-1} = \begin{bmatrix} w_j & y_j^* \\ y_j & w_j^* \end{bmatrix}$$

implies that

$$w_{j+1} = w_j(w_{j-1} + w_{j-1}^*) - w_{j-2} \tag{9a}$$

and

$$y_{j+1} = y_j(w_{j-1} + w_{j-1}^*) - y_{j-2} \; . \tag{9b}$$

The Fibonacci-sequence spectrum can be studied by applying periodic boundary conditions after j generations and examining the limit in which j gets large. The Bloch condition requires that

$$x_j \equiv \tfrac{1}{2}\,\mathrm{tr}\hat{T}_j = \mathrm{Re}(w_j) = \cos(Kd_j) \; , \tag{10}$$

where K is the Bloch wave vector and $d_j = F_{j-1}d_A + F_{j-2}d_B$ is the total length after j generations. From Eq. (9a) it follows that, as pointed out by Kohmoto,[17] the trace map is identical to that of the discrete models

$$x_{j+1} = 2x_j x_{j-1} - x_{j-2} \; , \tag{11}$$

and this implies that as j gets large the spectrum approaches a Cantor set. Thus the discrete and continuum cases are distinguished only by the starting conditions for the map and, in particular, by the invariant quantity[5,14]

$$I \equiv x_{j+1}^2 + x_j^2 + x_{j-1}^2 - 2x_{j+1}x_j x_{j-1} - 1 \; . \tag{12}$$

The fractal dimension of the spectral set becomes smaller and the range of scaling indices shifts to lower values as I becomes larger. Noting that $x_1 = \mathrm{Re}(u_B)$, $x_2 = \mathrm{Re}(u_A)$, and $x_3 = \mathrm{Re}(u_B u_A + v_B v_A^*)$, it can be shown that

$$I = [\mathrm{Re}(v_B v_A^*) - \mathrm{Im}(u_B)\mathrm{Im}(u_A)]^2 - [\,|v_B|^2 - \mathrm{Im}^2(u_B)][\,|v_A|^2 - \mathrm{Im}^2(u_A)] \; . \tag{13}$$

In the continuum model, I has a nontrivial dependence on electron energy which provides a useful characterization of the spectrum as we illustrate below.

The most general case we consider is one where each interval has subintervals of material 1 of width d_{1l} and d_{1r} on the left and right and a central subinterval of material 2 with width d_2. Then, choosing E_0 at the conduction-band minimum of material 1, V_1, an elementary calculation, yields

$$u_X = e^{-ik_1 d_{1,X}} \left[\cos(k_2 d_{2,X}) - i\sin(k_2 d_{2,X}) \left[\frac{k_1}{2k_2} + \frac{k_2}{2k_1} \right] \right] , \tag{14a}$$

$$v_X = i \left[\frac{k_2}{2k_1} - \frac{k_1}{2k_2} \right] e^{-ik_1(d_{1r,X} - d_{1l,X})} \sin(k_2 d_{2,X}) \; , \tag{14b}$$

where $d_{1,X} = d_{1r,X} + d_{1l,X}$, $E = \hbar^2 k_1^2/2m^* + V_1 = \hbar^2 k_2^2/2m^* + V_2$, and $X = A$ or B. For GaAs-$\mathrm{Ga}_{1-x}\mathrm{Al}_x\mathrm{As}$ systems we take $m^* = 0.068 m_0$, where m_0 is the electron mass and $|V_2 - V_1| = 134$ meV, corresponding to $x \simeq 0.2$. A situation similar to that of the discrete model with on-site energies alternating in a Fibonacci sequence (the diagonal model) may be realized by choosing the

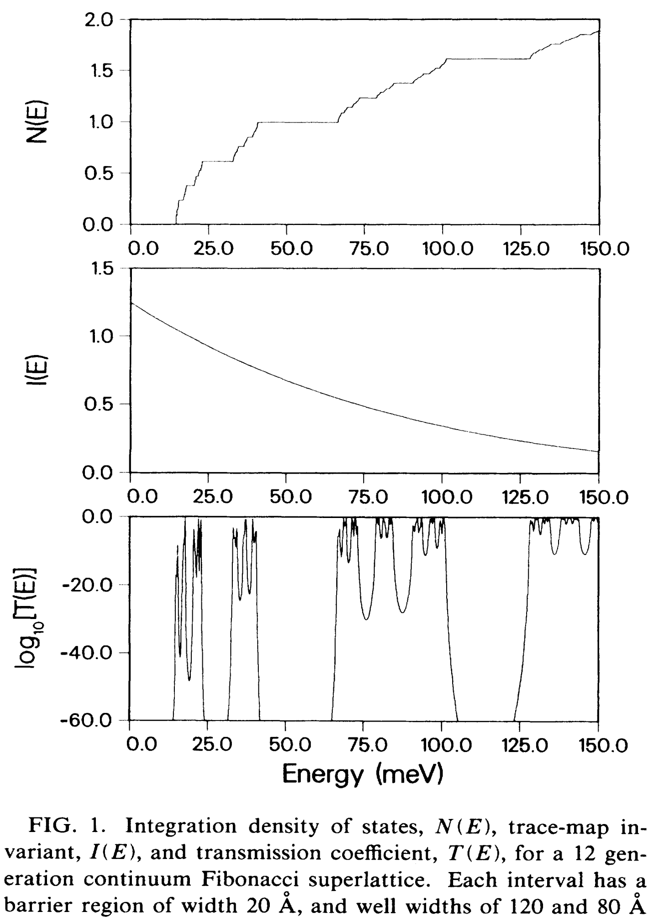

FIG. 1. Integration density of states, $N(E)$, trace-map invariant, $I(E)$, and transmission coefficient, $T(E)$, for a 12 generation continuum Fibonacci superlattice. Each interval has a barrier region of width 20 Å, and well widths of 120 and 80 Å are alternated in a Fibonacci sequences. $N(E)$ is in units of states per interval. For the corresponding discrete model $I = [(E_A - E_B)/2t]^2$ where the site energy for the narrow well, E_b, is larger and t is the hopping integral. Here I decreases with increasing E.

width of the barriers ($Ga_{1-x}Al_xAs$ regions) to be the same in A and B intervals but allowing the well widths (GaAs regions) to vary. Letting $d_{1r,A}=d_{1r,B}=0$, $d_{2,A}=d_{2,B}=d_2$, and inserting Eqs. (14) into Eq. (13) yields

$$I_D=\sin^2[(d_A-d_B)k_1)]\left[\frac{\kappa_2}{2k_1}+\frac{k_1}{2\kappa_2}\right]^2\sinh^2(\kappa_2 d_2)\ , \tag{15}$$

where we have assumed that $V_1<E<V_2$ and let $k_2=i\kappa_2$. [For wide high barriers ($\kappa_2 d_2 \gg 1$, $\kappa_2/k_1 \gg 1$) Eq. (15) can be shown to reduce to the corresponding expression for the discrete diagonal Fibonacci chain.] In Fig. 1 we show the spectrum resulting after 12 generations of the Fibonacci superlattice and $I(E)$ for barrier widths of 20 Å, $d_{1,A}=120$ Å, and $d_{1,B}=80$ Å. In Fig. 2 the spectrum after 12 generations and $I(E)$ are shown for $d_2=100$ Å, $d_{1,A}=24$ Å, and $d_{1,B}=16$ Å. Letting $\kappa_1=ik_1$ Eq. (15) becomes

$$I_{\rm OD}=\sinh^2[(d_A-d_B)\kappa_1]\left[\frac{\kappa_1}{2k_2}+\frac{k_2}{2\kappa_1}\right]^2\sin^2(k_2 d_2) \tag{16}$$

which can be shown to reduce to the expression given by Kohmoto and Banavar[5] for the off-diagonal discrete Fibonacci chain model in the appropriate limit.

The developments discussed above apply equally well for acoustic phonons in the continuum limit with the replacement $2m^*[E-V(x)]/\hbar^2 \rightarrow \omega^2/c^2(x)$, where $c(x)$ is the local sound velocity. Thus for acoustic phonons, k_1 and k_2 in Eqs. (14) are given by $k_1=\omega/c_1$ and $k_2=\omega/c_2$, and are always real.[21] In Fig. 3 we show the phonon spectrum and $I(\hbar\omega)$ for $d_{2,A}=0$, $d_{1,A}=60$ Å, $d_{2,B}=40$ Å, and $d_{1,B}=0$, where $c_1=4.72\times10^5$ cm s^{-1} (GaAs) and $c_2=5.62\times10^5$ cm s^{-1} (AlAs). In this case Eqs. (14) and (13) give

$$I=\left[\frac{k_2}{2k_1}-\frac{k_1}{2k_2}\right]^2\sin^2(k_1 d_{1,A})\sin^2(k_2 d_{2,B})\ . \tag{17}$$

Note that $I(\hbar\omega)$ vanishes like ω^4 as ω goes to zero, as in the discrete model.[5]

In closing, we comment on the transport properties of the continuum Fibonacci superlattice. The transmission coefficient for a j-generation Fibonacci superlattice is given by

$$T_j=|w_j|^{-2} \tag{18}$$

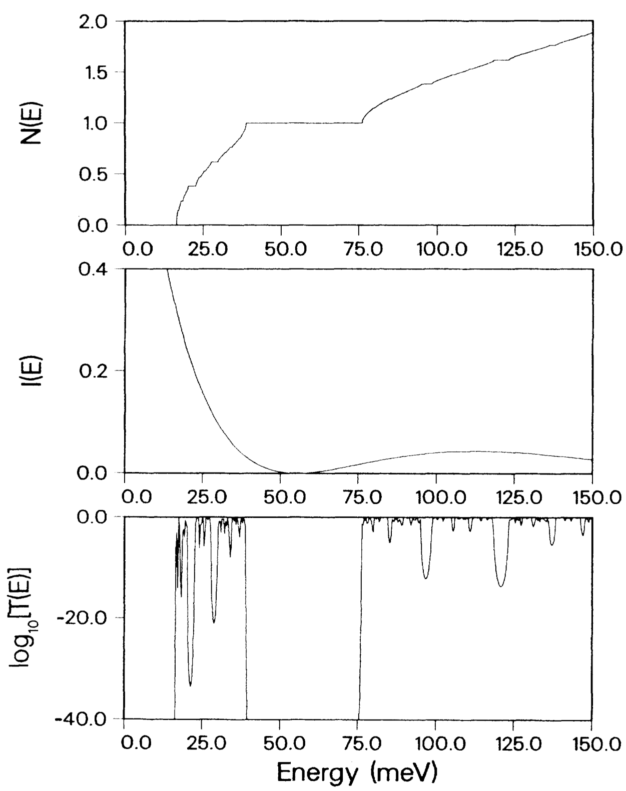

FIG. 2. As in Fig. 1 but for a Fibonacci superlattice with intervals of common well width (100 Å) and different barrier widths (24 and 16 Å).

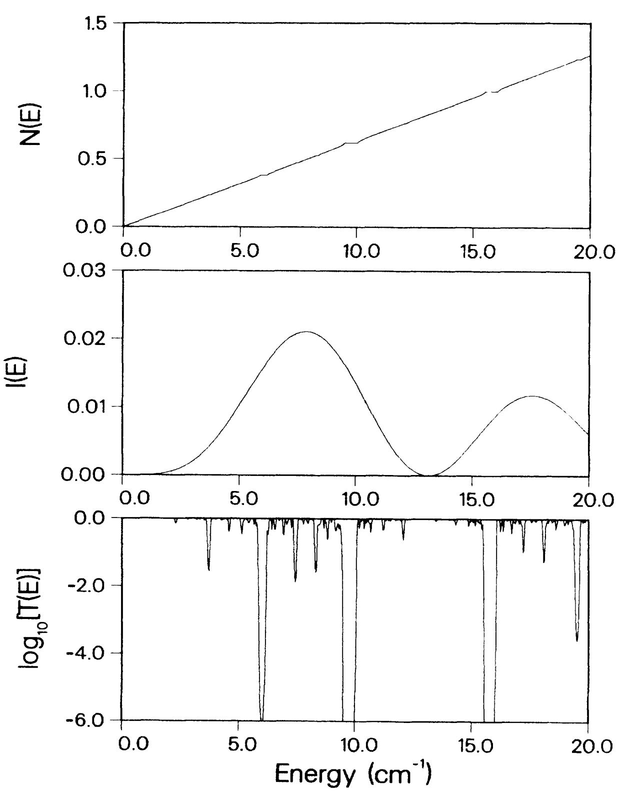

FIG. 3. As in Fig. 2 but for acoustic phonons ($E=\hbar\omega$) and A intervals composed of GaAs ($d_A=60$ Å) and B intervals composed of AlAs ($d_B=40$ Å). $I(E)$ vanishes whenever there is a resonance in either A intervals [$\sin(k_1 d_{1,A})=0$] or B intervals [$\sin(k_2 d_{2,A})=0$].

with w_j given by Eq. (9a). For electrons the conductance is related to T_j by the Landauer formula,[22] $G_j=(e^2/h)T_j/(1-T_j)$. For discrete models it has been conjectured[12,13] that for energies in the spectrum G_j decays as a power of d_j with a range of exponents, in accordance with expectations based on the nature of the spectrum. These conjectures can be firmly established in specific cases where the trace map is cyclic.[23] We do not believe that cyclic maps occur for the continuum model and numerical results for the dependence of transmission coefficients on length are similar to those for discrete models.[13] The dependence of the transmission coefficients on energy has been shown in the bottom panels of Figs. 1–3. The self-similar nature of the spectral set shows up more clearly than in plots of the integrated density of states. In Fig. 2 note that $T(E)$ tends to have larger values in the higher subband where $I(E)$ is smaller. In Fig. 3 we see that $T(E)=1$ at the energy where $I(E)$ goes to zero. This is associated with a resonance in material 2[$\sin(k_2 d_{2B})=0$] and is the analog for quasiperiodic systems of the property discussed by Tong[18] for random systems. As is apparent in Fig. 3 the scaling index of the spectrum goes to 1 when $I(E)$ goes to zero.

The authors acknowledge useful conversations with M. Kohmoto, R. Merlin, and B. Y. Tong.

---

*Present and permanent address: Physics Department, Indiana University, Bloomington, IN 47401.

[1]See Berry Simon, Adv. Appl. Math. **3**, 463 (1982), and references therein.

[2]D. Schectman, I. Bloch, D. Gratias, and J. W. Cahn, Phys. Rev. Lett. **53**, 1951 (1984).

[3]R. Merlin, K. Bajema, Roy Clarke, F.-Y. Juang, and P. K. Battacharya, Phys. Rev. Lett. **55**, 1768 (1985).

[4]D. Levine and P. Steinhardt, Phys. Rev. Lett. **53**, 2477 (1984).

[5]M. Kohmoto and J. R. Banavar, Phys. Rev. B **34**, 563 (1986).

[6]J. P. Lu, T. Odagaki, and J. L. Birman, Phys. Rev. B **33**, 4809 (1986).

[7]F. Nori and J. P. Rodriquez, Phys. Rev. B **34**, 2207 (1986).

[8]T. Odagaki and L. Friedman, Solid State Commun. **57**, 915 (1986).

[9]K. Machida and M. Fujita, Phys. Rev. B **34**, 7367 (1986).

[10]A. Mookerjee and V. A. Singh, Phys. Rev. B **34**, 7433 (1986).

[11]J. M. Luck and D. Petretis, J. Stat. Phys. **42**, 289 (1986).

[12]M. Kohmoto, B. Sutherland, and C. Tang, Phys. Rev. B **35**, 1020 (1987).

[13]T. Schneider, A. Politi, and D. Wurtz (unpublished).

[14]M. Kohmoto, L. P. Kadanoff, and C. Tang, Phys. Rev. Lett. **50**, 1870 (1983); M. Kohmoto and Y. Oono, Phys. Lett. **102A**, 145 (1984); L. P. Kadanoff and C. Tang, Proc. Natl. Acad. Sci. USA **81**, 1276 (1984).

[15]S. Ostlund, R. Pandit, D. Rand, H. J. Schellnhuber, and E. Siggia, Phys. Rev. Lett. **50**, 1873 (1983).

[16]For a recent review of the effective-mass approximation applied to multilayer semiconductor systems, see G. Bastard and J. A. Brum, IEEE J. Quantum Electron **QE-22**, 1625 (1986). Note that we are, to avoid inessential complications, ignoring the dependence of effective mass on position. Our work can easily be extended.

[17]M. Kohmoto, Phys. Rev. B **34**, 5043 (1986).

[18]See, for example, B. Y. Tong, Phys. Rev. A **1**, 52 (1970); Phys. Rev. **175**, 710 (1968).

[19]This is more explicit version of Eq. (2.11) in Ref. 17.

[20]$\{F_j\}$ are the Fibonacci numbers, $F_0=0$, $F_1=1$, $F_j=F_{j-1}+F_{j-2}$. After j generations there are F_j intervals in the Fibonacci sequence and $M_k=M_A$ or M_B according to the Fibonacci sequence. The quantities w_j and y_j are defined in terms of T_j by Eq. (8).

[21]We assume that, for the semiconductor superlattices of interest here, we can take the difference in local sound velocities to be due entirely to differences in the local mass density.

[22]R. Landauer, Philos. Mag. **21**, 863 (1970), D. C. Langreth and E. Abrahams, Phys. Rev. B **24**, 2978 (1981).

[23]B. Sutherland and M. Kohmoto (unpublished).